Chapter 2

Overview of Skeletal Repair (Fracture Healing and Its Assessment)

Elise F. Morgan, Anthony De Giacomo, and Louis C. Gerstenfeld

Abstract

The study of postnatal skeletal repair is of immense clinical interest. Optimal repair of skeletal tissue is necessary in all varieties of elective and reparative orthopedic surgical treatments. However, the repair of fractures is unique in this context in that fractures are one of the most common traumas that humans experience and are the end-point manifestation of osteoporosis, the most common chronic disease of aging. In the first part of this introduction the basic biology of fracture healing is presented. The second part discusses the primary methodological approaches that are used to examine repair of skeletal hard tissue and specific considerations for choosing among and implementing these approaches.

Key words Fracture healing, Radiography, Micro-computerized topography, Histomorphometry

1 Introduction: Overview of Fracture Healing

1.1 Bone Repair Recapitulates Embryological Skeletal Development

Fracture healing and bone repair are unique in that they are postnatal processes that mirror many of the ontological events that take place during embryological development of the skeleton (reviewed by refs. 1–5). Indeed many of the genes that are preferentially expressed in embryonic stem cells and the morphogenetic pathways that are active during embryonic skeletal development are also expressed in fracture callus and skeletal repair tissues [6, 7]. It is generally believed that the recapitulation of these ontological processes during fracture healing facilitates the regeneration of damaged skeletal tissues to their pre-injury structure and biomechanical function. In this regard, the interplay among regenerative processes in a number of different tissues—vascular, hematopoietic, and skeletal—is essential for the unimpeded repair of injured bones. Furthermore, the appropriate temporal differentiation of the various stem cell populations that form the different tissues and make up skeletal organs is dependent on the proper temporal spatial orchestration of specific paracrine, autocrine, and systemic signaling pathways [7, 8].

Matthew J. Hilton (ed.), *Skeletal Development and Repair: Methods and Protocols*, Methods in Molecular Biology, vol. 1130, DOI 10.1007/978-1-62703-989-5_2,

1.2 Fracture Healing Cascade

The cascade of events that is commonly described for fracture healing involves formation of a blood clot at the site of injury; an inflammatory phase in which specific cell types involved primarily in innate immune response participate; callus generation in which skeletal stem cells are recruited and differentiated into chondrocytes; primary bone formation in which stem cells are recruited to form bone; and secondary bone remodeling involving osteoclasts in which first mineralized cartilage and primary bone are resorbed followed by prolonged coupled remodeling. While these processes take place in a consecutive temporal manner, they overlap significantly and represent a continuum of changing cell populations and signaling processes within the regenerating tissue.

The disruption to the normal bone microenvironments that is caused by the fracture leads to the interactions of cell populations from the medullary space, periosteum, and enveloping muscular tissues. The signaling and cellular contributions from these different tissues and their microenvironments are unique and contribute to the heterogeneous nature of tissue formation at the fracture site [9]. Fracture healing and skeletal tissue repair broadly encompass an initial anabolic phase that is characterized by de novo recruitment and differentiation of skeletal stem cells that form a cartilaginous callus and, subsequently, of those that form the nascent blood vessels that will feed the new bone. This anabolic phase is followed by a very prolonged catabolic period encompassing resorption of the cartilaginous callus with its replacement by primary bone. Finally, the phase of coupled remodeling takes place, during which the marrow space and hematopoietic tissues are reestablished and regeneration of the original structural features of the injured skeletal organ is achieved. A temporal overview of the biological and histological events of fracture healing, the known cell types that are prevalent at each stage of fracture healing, and the stages at which specific signaling molecules are produced are presented in Fig. 1.

2 Assessing Skeletal Repair

2.1 Using an Integrated Approach to Assessing Tissue Repair

All skeletal healing can be defined both functionally (i.e., by the injured skeletal tissue's regain of its original structure and biomechanical properties) and in terms of the biological processes that facilitate the regain in function. Because of this complexity, an integrated approach should be taken to asses skeletal tissue repair at the level of the whole organ (via biomechanical and micro-computed tomography (μCT) assessments), at tissue and cellular levels (via histological assessments and some methods of contrast-enhanced μCT), and at molecular levels (via immunohistological, in situ hybridization, and other assessments of mRNA and protein expression) to define most clearly the mechanisms that promote healing. A description of the use of these techniques presented below

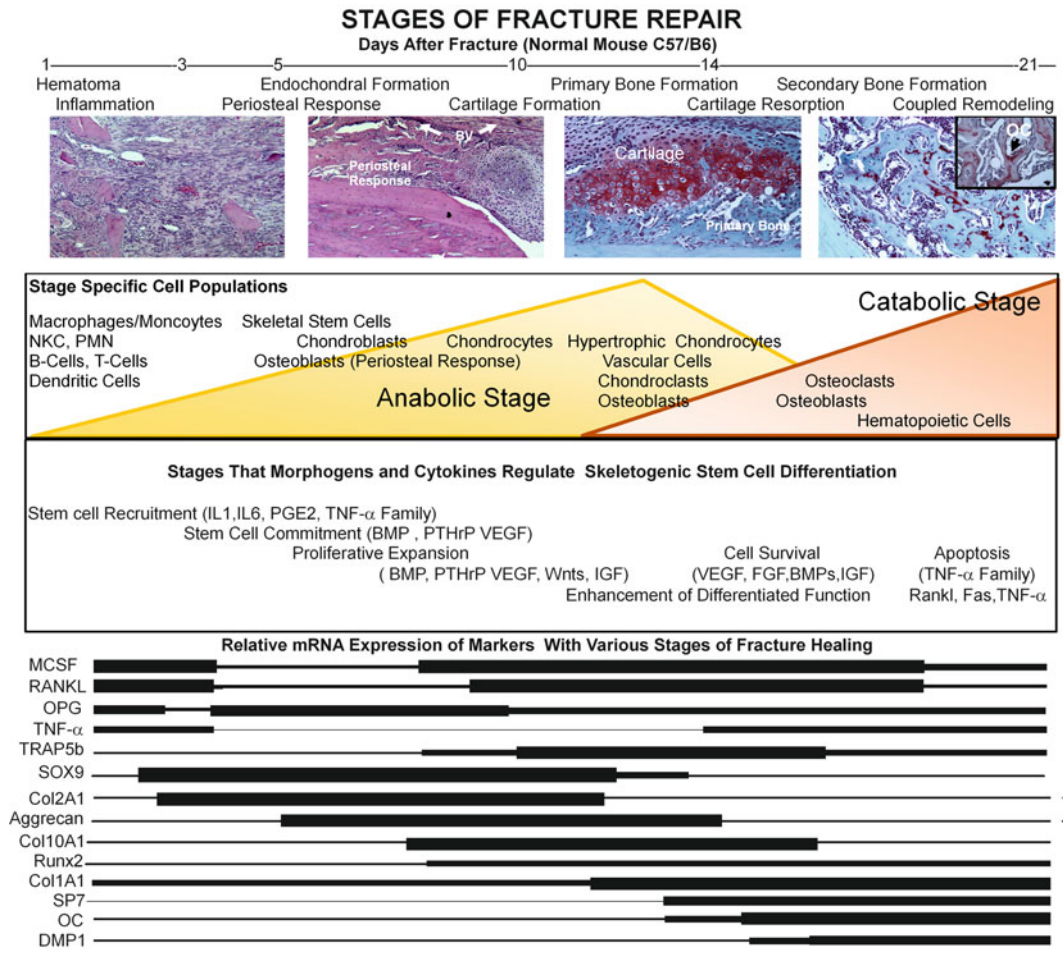

Fig. 1 Summary of the multiple stages of fracture healing. Summary of the stages of fracture repair and the timing of the development of these stages as seen in C57B6 strain of mouse is denoted at the *top* of the figure. Histological sections are presented *below* for each stage. All histological specimens are from sagittal sections of mouse tibia transverse fractures and were stained with H&E or Safranin-O and fast green; micrographic images are at 200× magnification. Section for the initial injury was taken from the fracture site 24 h post injury (*far left*). Sections depicting the initial periosteal response and endochondral formation are from 7 days post injury (*left middle*). *Arrows* denote blood vessels (BV) of the vascular in-growth from the peripheral areas of the periosteum. Sections depicting the period of primary bone and cartilage tissue resorption are from 14 days post injury (*middle right*). Sections depicting the period of secondary bone formation are from 21 days post injury (*far right*). Insert depicts 400× images of an osteoclast (chondroclast) resorbing an area of calcified cartilage. The major cell types associated with each stage and the relative time frames of the anabolic and catabolic stages of fracture healing are depicted by *yellow* and *orange triangular* overlays. The associated molecular processes and regulators next presented in the second *boxed area*. At the *bottom* of the figure, the levels of expression of various marker mRNAs for various molecular processes that have been examined in our laboratories are denoted by three *line* widths. The levels of expression are by percent over baseline for each and are not comparable between individual mRNAs. Data for expression levels for the pro-inflammatory cytokines and the ECM mRNAs were from Kon et al. [34] and Gerstenfeld et al. [4]

provides examples of how biological and functional characteristics are relatable to each other during the normal processes of fracture healing. Many of the methods described here in the context of fracture healing are also detailed in the various chapters of this book. Within this introduction a specific review is provided to illustrate how whole-organ and molecular assessments can be used in conjunction with the many other, tissue- and cell-based assays that are outlined in greater technical detail within the other chapters.

When considering the use of multiple assessments, it is important to recognize that performing several assessments on the same sample can be advantageous from the standpoint of cost savings and statistical power. For example, following μCT imaging with mechanical testing allows direct examination of relationships between mechanical behavior and both structure and mineralization. With this particular sequential approach, one can also use the measured mechanical properties to provide an important calibration or validation of finite element models created from the μCT data [10]. Alternatively if the tissue is first fixed, such as with formalin, μCT imaging can be followed by histological assessments. This sequence allows one to relate cellular composition to structure and mineral content. Use of multiple approaches may also be used as a means of validating biological and structural findings. As an example, qRT-PCR analyses of mRNA expression of markers of chondrogenesis or osteogenesis or osteoclastogenesis may be used to confirm histological and histomorphometric data of cartilage and bone compositions as well as to define the remodeling and developmental progression of these tissues. By assessing bone healing at multiple levels (organ, tissue, cellular, and molecular) relationships and interactions between the various mechanisms that work at each level during fracture healing can then be developed. A summary of the most common measurements that are made in the assessment of skeletal repair tissues is presented in Table 1.

2.2 Selection of a Model to Assess Skeletal Repair

The model that one chooses to use in assessing skeletal tissue repair should be carefully considered in relationship to the research questions that are being asked. In this context four considerations come into play:

1. If one is using a surgical model as a means of extrapolating developmental and regenerative characteristics about skeletal tissues, the nature of the type of skeletal formation process that one wishes to examine (intramembranous bone formation versus endochondral bone formation) is important to consider.
2. The nature of both the bone (cortical versus intermedullary) and the surrounding soft tissue compartments that are effected and contribute to the repair process should be considered.
3. The skeletal organ and its developmental background should be considered. At its simplest level this would divide surgical

Table 1
Metrics of bone repair

	Units
(a) Radiographic data	
Faxitron radiography	
Areal BMD	Gray level
Projected bone area	μm^2
Computed tomography	
Total callus volume	mm^3
Mineralized callus volume	mm^3
Mineralized callus volume fraction	–
Callus mineral content	mg HA/cm^3[a]
Average tissue mineral density	mg HA/cm^3[a]
Standard deviation of tissue mineral density	mg HA/cm^3[a]
(b) Biomechanical data (torsion)	
Ultimate torque	N mm
Torsional stiffness	N mm/°
Torsional rigidity	N mm^2/°
Twist to failure	°
Toughness (work to failure)	N °
(c) Histomorphometric data[b]	
Callus diameter (CDm)[c]: Mean value for measurements made, in two orthogonal planes, of the diameter of the midpoint of the fracture callus	Mm
Total callus area (CAr): Mean value for measurements of the total callus areas inclusive of all tissues both within and outside the original bone cortices	mm^2
Area of cartilage (Cg/Ar): Mean value for measurements of the total cartilage in the callus. May alternatively be expressed as the percent of total callus volume that is cartilage (%Cg)	mm^2
Area of total osseous tissues TOT/Ar: Mean value for measurements of total callus area that is osseous tissue (includes preexisting cortical bone, new woven bone, and surfaces lined by osteoblasts). May alternatively be expressed as the percent of total callus volume that is osseous tissues (%TOT)	mm^2
Area of void (V/Ar): Mean value for measurements of total callus area that includes the marrow cavity, hematopoietic elements, and empty unstained space. May alternatively be expressed as the percent of total callus volume that is the void (%V)	mm^2
Area of fibrous tissue FT/Ar: Mean value for measurements of traced areas of fibrous tissue within the callus. May alternatively be expressed as the percent of total callus volume that is fibrous tissue (%FT)	mm^2
Osteoclast volume density (Oc/Ar): Mean value for measurements of tartrate-resistant acid phosphatase-stained cells calculated as the number of osteoclasts per unit area of callus	(#/mm^2)
Osteoblast bone surface density (Ob/Ar): Number of osteoblasts lining a bone or a mineralized cartilage surface as calculated per unit surface area of new trabecular bone	#/mm^2
Number of vessels per callus area	(#/mm^2)

[a] *HA* hydroxyapatite. While area, diameter, and cartilage values are not listed in Table 1 and are not commonly used measurements in metabolic bone studies they are defined and their nomenclature as is in the original agreed standard

[b] *Relational determinations to biomechanical testing*. CDm and CAr measurements provide comparative values to X-ray, qCT, and biomechanical determinations. Diameters can be used in calculations of moments of inertia. C:TOT measurements can be used in material assessments in relationship to stiffness and strength determinations. Vd: Since the external callus tissue initially is devoid of a hematopoietic containing marrow space the assessment and the progression of Vd area gives total measurements of rates of resorption and subsequent remodeling of the external callus and may be related to OcD

[c] Values in parenthesis () denote nomenclature as is in the agreed standard[2]

models into those that assess bone repair in appendicular, axial, and cranial tissues or in different soft tissue elements.

4. If one is assessing a therapeutic modality the surgical model that is chosen should most closely approximate the orthopedic application and therapeutic modality that is being assessed.

It is also important to note that, due to the effects of systemic interactions and the heterogeneity in cellular composition, in vivo models cannot be used to fully dissect the molecular mechanisms of the various biological processes that effect repair. It is therefore ideal that in vivo studies should be complemented with in vitro methods of cell or organ culture that are presented in this book.

A fracture or any surgical repair model may be tracked temporally and isolated spatially. In the case of a fractured long bone, the injury induces one round of endochondral bone formation in which callus cells differentiate in a synchronous manner that temporally phenocopies the spatial/temporal variation of the cell zones from the top to the bottom of the growth plate. This round is followed by a prolonged period of coupled remodeling. Fracture healing therefore, represents an ideal biological process to examine in a postnatal context many cellular and molecular mechanisms that underlie both the endochondral bone formation that takes place during skeletal tissue development and the coupled remodeling that takes place during skeletal tissue homeostasis.

3 Whole-Organ Assessments

The two central, functional attributes of skeletal tissues are their ability to regulate apatite mineral deposition and resorption and to assemble and model the microstructure of the mineralized tissue to meet the biomechanical needs of the animal. These unique functional attributes make radiographic approaches particularly useful in examining skeletal tissue repair since these approaches focus on the mineralized tissues within the callus.

3.1 Plain-Film X-Ray

This assessment is the most common clinical tool to assess hard tissue repair, although this assessment is limited by its relatively qualitative nature [11–13]. Figure 2 presents a series of plain-film X-ray assessments made across a time course of fracture healing. This type of study provides a first approximation of the progression of tissue repair (Fig. 2). For these studies, an X-ray device with a high-energy beam and capability of high resolution, such as a Faxitron® cabinet X-ray system, is ideal. The best resolution is obtained if the bone is removed from the animal and cleaned of a large amount of surrounding soft tissue. Fixation devices should be left in place to maintain the integrity of the construct up until the tissue construct is stable. At least two separate anatomical orientations

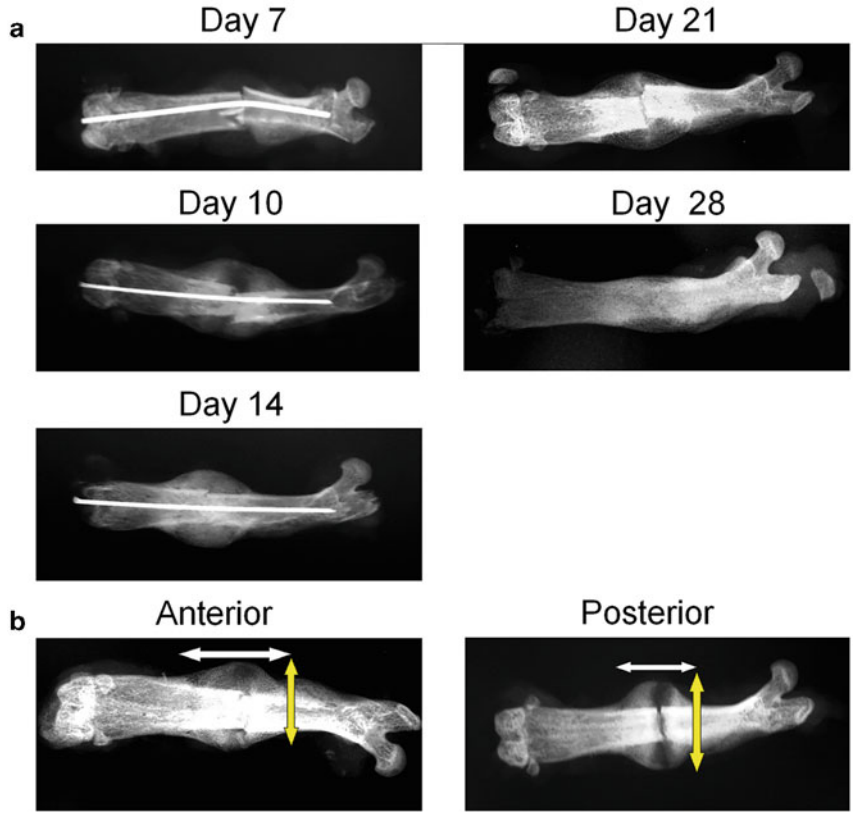

Fig. 2 Radiographic series for assessment of fracture healing. (**a**) Time series of evolution of mouse femur fracture callus structure and mineral content. (**b**) Anterior and posterior views of mouse femur fracture callus at 10 days post fracture. All images were produced with a Faxitron® device set at 40 s and 30 kV

should be used to make such measurements of callus dimensions and bone bridging since the tissues that form during repair can be irregular in shape and cortices of most bones are not true cylindrical structures.

3.2 μCT

Given that the size, shape, and composition of the bone repair tissues change over the time course of healing, μCT can provide important, qualitative, and quantitative assessment of these changes so as to provide nondestructive, and even noninvasive, evaluation of repair progress. We and others have developed "standard" methods of μCT evaluation of mineralized tissues in fracture healing as well as contrast-enhanced μCT methods for examining contributions of non-mineralized tissues and vascular elements.

3.2.1 μCT Assessment of Mineralized Tissues in the Callus

Many of the technical considerations for μCT studies of intact bones [14] also apply to studies of fracture healing. These considerations include scanning parameters (voltage, current, integration

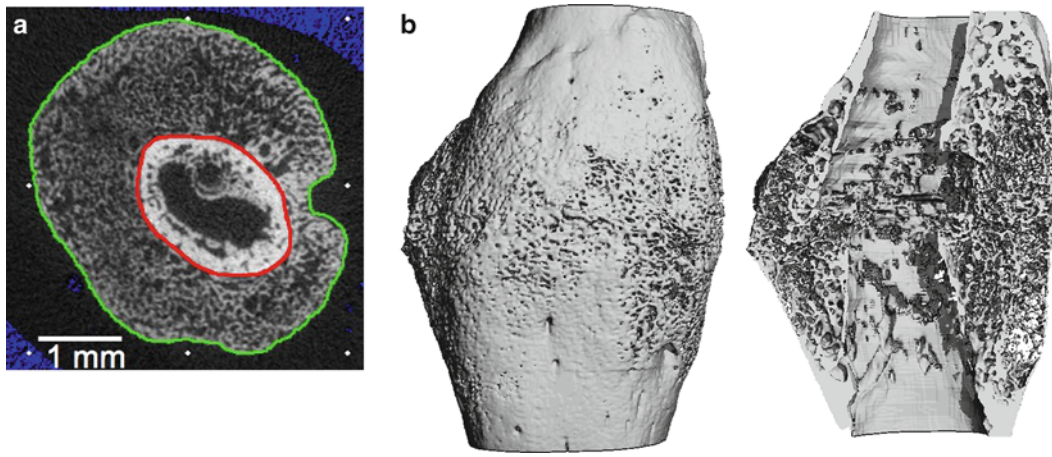

Fig. 3 (**a**) Definition of the outer (*green*) and inner (*red*) callus boundaries on a transverse cross section of micro-computed tomography scan of a fracture callus at 14 days post fracture. (**b**) The 3-D volume of interest that is defined by the area enclosed by these two boundaries on each transverse cross section along the length of the callus is shown rendered in entirety on the l*eft* and in a longitudinal cutaway view on the *right*. Reprinted from Morgan et al. [15]

time, and resolution) and methods of image processing (noise filtering, thresholding, and defining volumes of interest for analysis). Typically, image resolutions of 16 and 12 μm/voxel are sufficient for rat and mouse calluses, respectively. A Gaussian filter is also commonly used. These resolutions and filter are standard for commercially available desktop μCT systems.

The boundaries of the callus must be defined in μCT assessments, if one is interested in quantifying callus size and fraction or percentage of the callus occupied by mineralized tissue, just as described below for histomorphometric assessments of callus tissues. Identification, or *segmentation*, of the callus can be achieved by defining the outer and inner boundaries of the callus on transverse cross-sectional images distributed along the length of the callus (Fig. 3). Although we often use an inner boundary that excludes the cortex and medullary space, this boundary can be omitted for complete analysis of the extent of bridging (since some bridging of the cortex might be present), and if healing is so advanced then the boundary between the cortex and mineralized callus tissue cannot be reliably identified.

Upon defining the callus or some portion of the callus as the volume of interest, one needs to choose one or more thresholds for specific quantification and visualization of the mineralized portions of the callus. A threshold is a gray value above which a voxel in the μCT scan will be considered to contain mineralized tissue. If a simple categorization of mineralized vs. unmineralized tissue is desired, then one threshold is sufficient. If three or more categories of the relative extent of mineralization are desired, or if a scaffold

or an implant material is present, then more than one threshold may be used. At present, there is no standard method for choosing a threshold. We recommend that regardless of how many thresholds are used, a threshold should be defined as a percentage of the average gray value of the preexisting cortex or implant material [15]. Although commercial μCT systems have software algorithms for quantifying trabecular structure, this type of analysis is not appropriate for repair tissues, because the wide range of mineralization that is present in these tissues renders the measures of "trabecular" thickness, "trabecular" number, connectivity, etc. extremely sensitive to the choice of threshold.

A number of outcome measures can be quantified using μCT (Table 1). Some of these measures describe callus size and quantity of mineralized tissue (total volume, mineralized volume, mineralized volume fraction, mineral content), while others describe the mineralization (average and standard deviation of the tissue mineral density) or the overall structure (moment of inertia).

3.2.2 Contrast-Enhanced μCT Imaging of Cartilaginous Tissues in the Callus

Formation of the cartilage tissues is a key phase of many skeletal tissue studies. During skeletal repair, cartilage tissues provide initial stability at the surgery or fracture site and serve as a template for subsequent formation of mineralized tissue. In order to provide nondestructive assessment of the soft callus with μCT, a contrast agent is required to increase the X-ray attenuation of these tissues. We have used a cationic, iodinated contrast agent [16] for this purpose. On account of the large, fixed negative charge in cartilage, the contrast agent, via electrostatic attraction, preferentially accumulates in regions of cartilage within the callus. These regions incur the largest increase in attenuation from pre- to post-incubation images. The attenuation of the non-cartilaginous soft tissues is moderately increased, allowing clear delineation of the callus boundaries, while the attenuation of bone tissue is unchanged. The basic experimental approach in this contrast-enhanced μCT (CECT) method is to perform μCT scans both before and after incubation of the callus in the contrast agent (Fig. 4a). Analysis of the preincubation images, post-incubation images, and images formed by subtracting the former from the latter enables discrimination among cartilage, non-cartilaginous soft tissue, and mineralized tissue in the callus. The respective locations of these different tissues within the callus can be nondestructively visualized and quantified in both 2-D and 3-D (Fig. 4). Measurements of callus area and cartilage area made with CECT compare well to those made using histomorphometry (Fig. 4c–e).

3.2.3 Contrast-Enhanced μCT Imaging of Vessel Structure in the Callus

A different contrast agent that is perfused at the time of euthanasia allows μCT assessment of the vasculature during bone repair. In this method, a contrast agent such as a mixture of lead chromate and silicone rubber (Microfil MV-122; Carver, MA) is injected

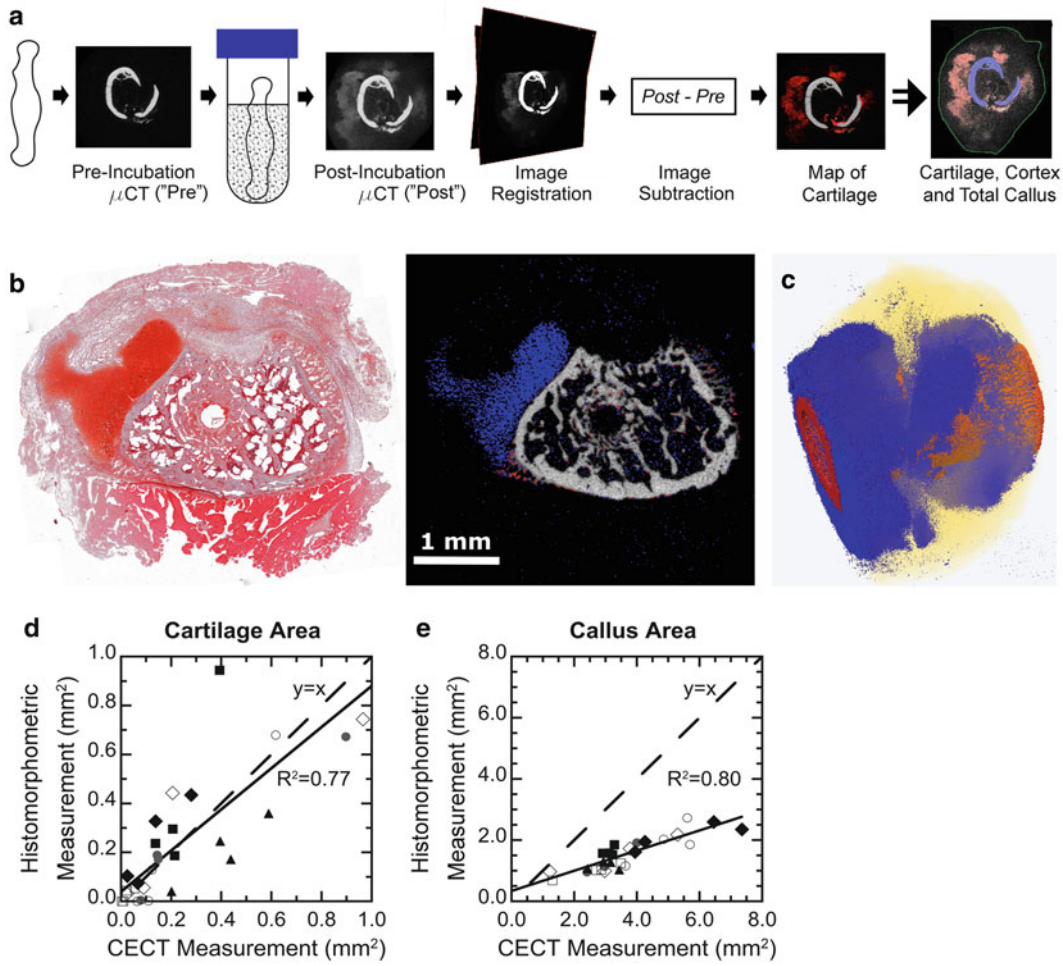

Fig. 4 (**a**) CECT method: Labeling of tissues in the *far right* image is as follows: callus boundary = *green* outline; cartilage = *red*/*pink*; cortex = *purple*; other mineralized tissue = *grey*. (**b**) Comparison of (*left*) a histological section (*bright orange-red* = cartilage) and (*right*) CECT cross section (*blue* = cartilage; *red* = mineralized cartilage; *grey* = bone) of a murine fracture callus (postoperative day 10). (**c**) 3-D rendering of a callus imaged with CECT (*red* = cortex; *blue* = cartilage; *yellow* = non-cartilaginous soft callus). Comparison of histomorphometric and CECT measurements of (**d**) cartilage area and (**e**) total callus area. Each symbol represents a different callus ($n = 4$ measurements per callus, each corresponding to one quadrant of the cross section)

through the left ventricle of the heart and allowed to perfuse with drainage into the body cavity by cutting the vena cava. After perfusion the contrast agent is allowed to polymerize [17, 18]. The choice of contrast agent and imaging procedure depends on the type of CT scanner available and the type of vasculature to be quantified [19]. For imaging of only intermediate- to large-sized vessels or when using synchrotron μCT, a very highly attenuating contrast material, such as bismuth [20], could be used and discrimination between the contrast-enhanced vascular casts and the

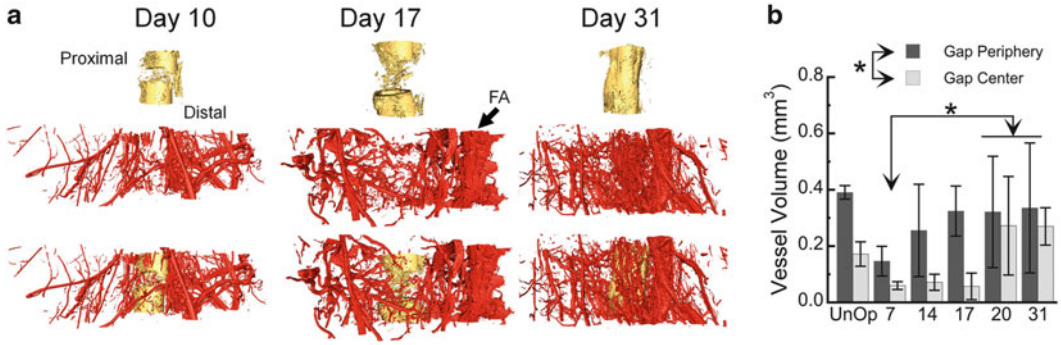

Fig. 5 (**a**) 3-D renderings of the mineralized tissue (*yellow*) without (*top row*) and with (*bottom row*) the vasculature (*red*) in calluses from a murine model of distraction osteogenesis (DO). "FA" denotes femoral artery. (**b**) Vessel volume in the gap periphery vs. gap center for the DO time course and unoperated controls (*$p < 0.05$). Reprinted from Matsubara [44] and Morgan [19]

surrounding mineralized tissue can be achieved purely with a threshold [21–23]. However, for analyses of small vascular elements using a desktop μCT system, only a μCT scan performed after decalcification of the host bone is likely to allow clear discrimination between vessel and mineralized tissue.

The disadvantages of performing the μCT scan after decalcification are twofold. First, decalcification results in large changes in shape and size of the callus, and the original anatomic positions of the vessels are thus lost. Second, the spatial relationship between vascular elements and mineralized tissue cannot be determined. An extension of the aforementioned method is to perform μCT scans both before and after decalcification. The post-decalcification images are registered to and then subtracted from the pre-decalcification images to yield data on the vessels (in their original anatomic position), mineralized tissue, and the respective locations of these two tissues (Fig. 5).

3.3 Mechanical Approaches

In the laboratory setting, the mechanical properties of a healing bone are also commonly assessed by mechanical tests that load the bone in torsion or in three-point bending. The choice of the type of test is dictated by technical as well as physiological considerations. Tension and compression tests are not commonly used, because variability in the alignment of the fracture and in the asymmetry of the callus will lead the applied tensile or compressive displacements to induce variable amounts of bending and shear within the callus. Bending and torsion are logical choices when studying fracture healing in long bones, because these bones experience bending and torsional moments in vivo. However, whereas torsion tests subject every cross section of the callus to the same torque, three-point bending creates a nonuniform bending moment throughout the callus. As a result, failure of the callus

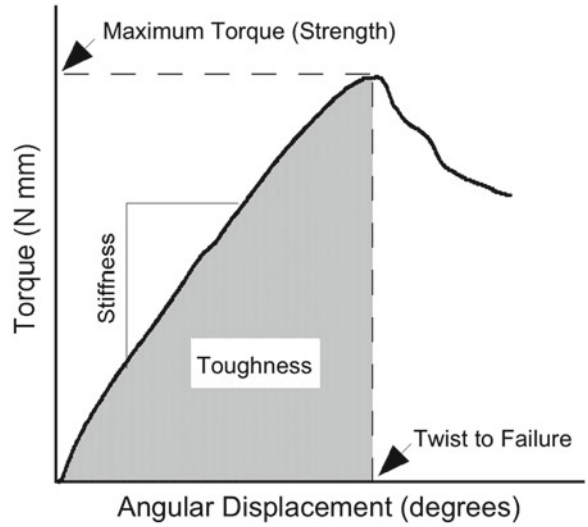

Fig. 6 Representative torque-twist curve for a mouse tibia 21 days post fracture. The curve is annotated to show definitions of basic biomechanical parameters. Torsional rigidity is computed by multiplying the torsional stiffness by the gage length. Analogous definitions hold for bending tests

during a three-point bend test does not necessarily occur at the weakest cross section of the callus.

Regardless of the type of mechanical test, the outcome measures that can be obtained are the strength, stiffness, rigidity, and toughness of the healing bone (Fig. 6). For torsion tests, an additional parameter, twist to failure, can be used as a measure of the ductility of the callus. Although strength, a measure of the force or the moment that causes failure, can be measured only once for a given callus, it is possible to obtain more than one measure of stiffness and rigidity. Multistage testing protocols have been reported that apply nondestructive loads to the callus in planes or in loading modes that are different from those used for the stage of the test in which the callus is loaded to failure. With these protocols, it is possible to quantify the bending stiffness in multiple planes [24] or the torsional as well as compressive stiffness [25].

The mechanical properties illustrated in Fig. 7 are structural, rather than material, properties. *Material properties* describe the intrinsic mechanical behavior of a particular type of material (tissue), such as woven bone, fibrocartilage, or granulation tissue. The *structural properties* of a fracture callus depend on the material properties of the individual callus tissues as well as the spatial arrangement of the tissues and the overall geometry of the callus. While it is possible to use measurements of callus geometry together with those of structural properties to gain some insight into callus tissue material properties [26] true measurement of these material properties requires direct testing of individual callus tissues [27, 28].

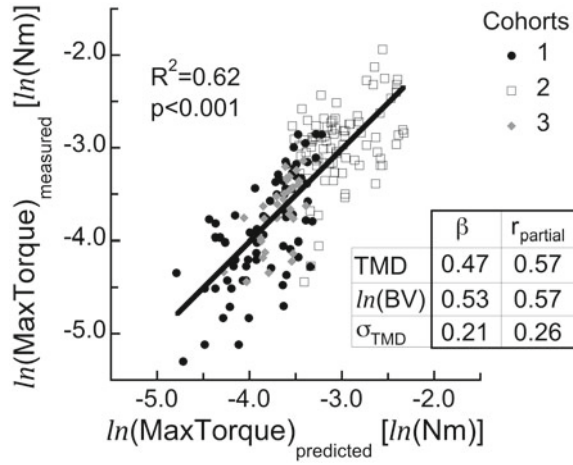

Fig. 7 Prediction of torsional strength by BV, TMD, and σ_{TMD}. The beta weight (β) and partial correlation coefficient ($r_{partial}$) are given for each μCT measure to indicate its relative contribution. Data from Kakar et al. [37]

Although there is no substitute for mechanical testing to assess the extent of healing at intermediate-to-late time points, it is of biological and translational interest to identify relationships between the mechanical properties of the callus and nondestructively obtained measurements of callus composition and structure. In a large, composite dataset of murine calluses at multiple time points post fracture [15], torsional strength was best predicted (as determined by stepwise regression) by the combination of average tissue mineral density, mineralized callus volume, and standard deviation of mineral density ($r^2 = 0.62$, $p < 0.001$) (Fig. 7, Table 1). Torsional rigidity was best predicted by the combination of average tissue mineral density, callus mineral content, mineralized volume fraction, and standard deviation of mineral density ($r^2 = 0.70$, $p < 0.001$). Changes in the calluses over time were characterized primarily by an increase in average tissue mineral density, while variability among calluses at a given time point was seen primarily in the measures that quantify the absolute and relative amounts of mineralized tissue in the callus, i.e., mineralized callus volume, callus mineral content, and mineralized volume fraction. Overall, these results illustrate how the mechanical properties of the callus depend on measures of both the quantity and mineral density of the hard tissue.

4 Tissue-Level Histological Approaches

Of the recommendations and conventions defined by Parfitt et al. [29] for general histological assessments of skeletal tissue, we have put forth our perspective on the aspects of these assessments that

would be most appropriate for bone repair [30]. Extensive details of histological methods including in situ hybridization and immunohistochemistry are discussed in other chapters in this book and are not discussed in detail here. Rather, the present focus is on general recommendations as to how to approach the use of histological and histomorphometric approaches in the analysis of fracture callus tissues. It is important to note that repair tissues are very heterogeneous, being composed of cartilage, bone, fibrous, and hematopoietic tissues, which are changing throughout the repair process. Therefore, the greatest challenge confronting any histological assessment of a bone reparative process is how to sample this heterogeneous tissue so that any quantitative measurements are representative of the repair tissue that is formed.

In this regard two sets of issues should be considered in any histological assessment of skeletal repair tissues. The first is related to the anatomical plane and sampling of the repair tissue. While fracture calluses may be examined in a longitudinal plane such approaches provide primarily a qualitative overview of the tissue heterogeneity. This in part is due to difficultly of reproducibly positioning a bone during embedding such that a uniform longitudinal plane is always sectioned between individual specimens. This problem largely is related to the fact that long bones are not perfectly cylindrical as illustrated by comparisons of the anterior and posterior X-ray images in Fig. 2b and the MicroCT reconstructions presented in Fig. 3b. Sampling of tissue compositions is further complicated by the fact that endochondral bone formation, and cartilage resorption and bone remodeling that occur during tissue repair, arises also in a nonuniform manner. This is underscored by Fig. 8, which presents the immense structural heterogeneity in representative longitudinal and transverse sections of fracture calluses at 14 days post injury. To address this challenge, transverse sections can be collected at fixed increments along the long axis of the callus. This sectioning approach provides an optimal means for both observing the variability of the tissue formed in all three planes of the callus and obtaining accurate cross-sectional diameters and area measurements at precisely defined anatomical positions within the callus and in relationship to the fracture site. We have used serial sections to reconstruct in three dimensions the tissue compositions of whole calluses [31] and to obtain measurements of the mechanical properties of callus tissues in conjunction with histological assessment [27].

The second practical aspect to be considered in the application of histomorphometric techniques to bone healing studies is to identify appropriate histological stains to assess the callus. It is important to recognize that a tissue stain should not be used to determine tissue phenotype but rather to improve and enhance visualization of that tissue by distinguishing it, by color, from a

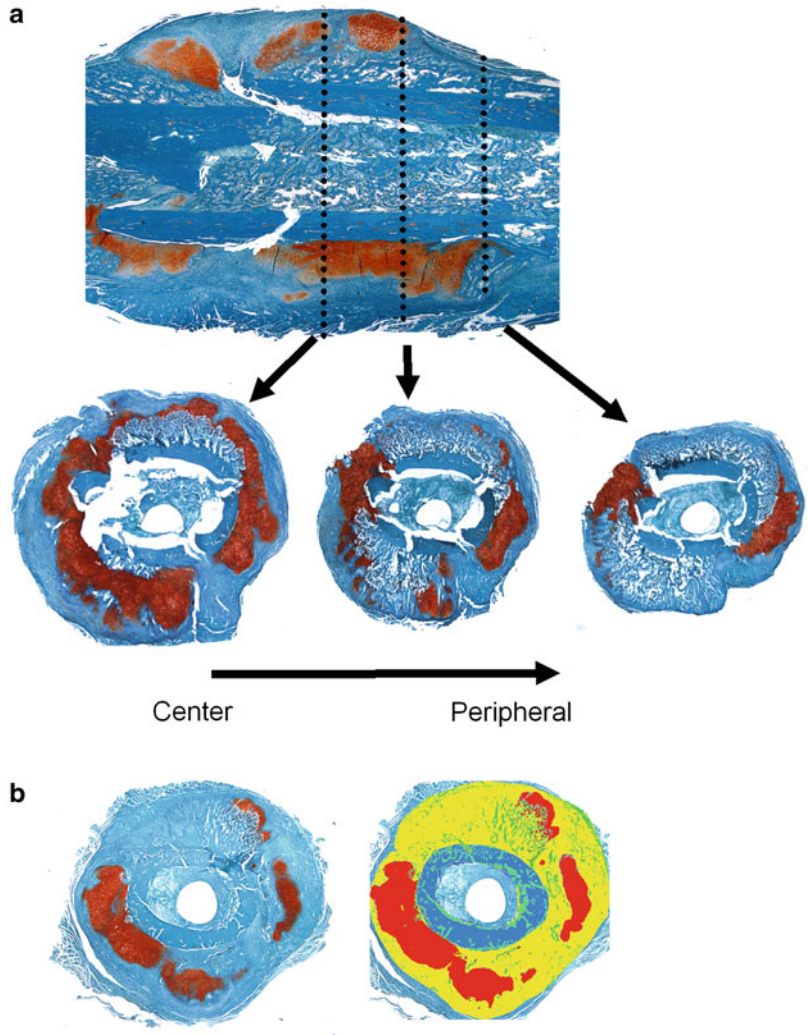

Fig. 8 Histological approach to assess fracture. (**a**) Demonstration of the tissue heterogeneity and morphological irregularity of both the longitudinal and transverse dimensions. Three transverse slices taken from *center* at three increments from the *center* to *edge* of the callus showing how the cartilage content varies. (**b**) Demonstration of pseudo-coloring of Safranin-O/fast green-stained sections segmenting cartilage from voids and bone areas

different histologically contiguous tissue. Multiple stains can be used to discriminate cartilage from bone and have been used in studies assessing fracture healing. In our studies we have used Safranin-O/fast green staining, which has been widely used and shown to be effective in measurements of cartilage thickness in studies of osteoarthritis [32] and to quantify the amount of cartilage tissue repair of joint surfaces [33]. Other studies also have used combinations of alcian blue with hematoxylin and eosin in order to obtain differential staining of cartilage and bone [34, 35].

In general, a staining protocol should provide consistent staining outcome that will enhance histological tissue discrimination of cartilage from bone and non-osseous tissue and can be used with semiautomated measurement techniques.

5 Molecular Approaches

The assessment of the expression of mRNAs in conjunction with immunohistochemical approaches provides a means of identifying the underlying morphogenetic signaling and regulatory processes that regulate bone repair. In this final section three separate approaches to assay mRNAs (in situ hybridization, individual candidate mRNA assays, and large-scale microarray) are discussed.

5.1 In Situ Hybridization

At the single mRNA level in situ hybridization is used to identify the nature of specific cell populations and their anatomical localization within the callus surrounding muscle and marrow spaces that are expressing a given mRNA. Such approaches can be used both to identity and to validate simple histological assessments of the cell type (chondrocytes, osteoblasts, etc.) and the differentiated states of these cells [31]. This approach can also be used in conjunction with immunohistological methods to place in anatomical context the cells expressing a given regulatory factor or morphogenetic protein relative to those expressing receptors that make them responsive to these signals.

5.2 Individual mRNA Assessments

Isolation of total RNAs from the entire callus allows one to look at the expression of individual mRNAs within the total cell population of the callus tissue. This approach can be used to provide an extremely sensitive temporal road map of the differentiation and development of the tissues and cell types of the callus as well as the expression or any regulatory factors that one is interested, which may be functional in fracture healing. It is critical that calluses be isolated quickly and in as reproducible manner devoid of surrounding muscle as possible with manual dissection methods. Tissues should be dissected as exactly as possible from the point the callus initially rises from cortical surface, and since it is physically impossible to separate the original bone and marrow elements from the external callus we isolate the mRNAs from the intact tissue specimen. At very early time points before the callus has condensed (day 5 for mouse and day 7 for rat) a margin of muscle may be needed to ensure that the early regenerative cells are isolated, but some caution should be taken to interpret the anatomical localization of the cells that are expressing a given mRNA species. Confirmatory analysis using in situ hybridization or immunohistochemistry is recommended.

It is important to note that there are some differences of opinion on how to assess replicates. For our studies in mouse, we generally use three biological replicates, each representing a pool of total RNAs from calluses of three animals. Reference mRNAs are made from unfractured bones (three replicates pooled from groups of three animals) isolated from the mid-diaphyseal region of these bones. This approach incorporates aspects of obtaining reproducibility from assaying replicates and takes into account biological variability since the replicates represent experimental repeats of multiple pooled animal samples. We have taken this approach since mRNA yields from single-mouse calluses are very small and insufficient to carry out assays for large numbers of genes or for use in microarray studies. In general this approach has provided a very sensitive means of seeing reproducible differences in temporal profiles of expressed genes under differing experimental conditions [34, 36, 37]. For studies performed in rats, individual calluses provide sufficient yields of total mRNA for running multiple mRNA assays [38].

5.3 MicroArray Approaches

Sequencing of the entire genomes of multiple species has provided the means by which the transcriptome of fracture healing can be assessed by microarray analysis. Given the expense of such studies these approaches should only be carried out in conjunction with a core facility that has technical staff, instrumentation, and a track record of executing this type of study. The setup of a microarray study involves a number of crucial steps; the first and most important is to have sufficient replicates per experimental group (treatment condition or animal genotype, and time point). In planning a study, sufficient RNA is needed to carry out the array twice in the event of a technical problem with the execution of the array and to carry out mRNA candidate validation by qRT-PCR. A minimum of three biological replicates is recommended as described above. Analysis of microarray data should follow four main steps: (1) quality control to identify microarray artifacts from hybridization and correct for chip batch effects, (2) data pre-processing to eliminate outliers, (3) identification of differentially expressed genes (DEG), and (4) extraction of biological knowledge from DEG. It is recommended that, given the expense of microarray experiments, appropriate expertise in statistical and computational analysis also be available either through collaborative or fee-for-service arrangements. The most basic approach in **step 3** uses basic statistical analysis to identify genes that showed the greatest quantitative changes in their expression [39–41]. In this context this type of approach can be used to identify both known and novel genes that show the greatest changes in expression over the time course of healing. Other more sophisticated statistical approaches have been carried out that cluster genes based on common temporal profiles of expression and that examine gene functions in each cluster across the time course of fracture healing [6, 42, 43].

6 Conclusion

In this brief introductory chapter we have reviewed the biological events of fracture repair. We have also laid out a number of general methodological approaches including a summary of various radiographic and molecular techniques that are used to assess bone repair, using fracture healing as the example. General guidance is presented on integrating multiple technical approaches to best assess skeletal repair that may also be applicable for other areas of skeletal biology research.

Acknowledgments

This work is supported by NIH Grants AR056637 and AR062642.

References

1. Bolander ME (1992) Regulation of fracture repair by growth factors. Proc Soc Exp Biol Med 200(2):165–170
2. Einhorn TA (1998) The cell and molecular biology of fracture healing. Clin Orthop Relat Res 355(Suppl):S7–S21
3. Ferguson C et al (1999) Does adult fracture repair recapitulate embryonic skeletal formation? Mech Dev 87:57–66
4. Gerstenfeld LC et al (2003) Fracture healing as a post-natal developmental process: molecular, spatial, and temporal aspects of its regulation. J Cell Biochem 88(5):873–884
5. Vortkamp A et al (1998) Recapitulation of signals regulating embryonic bone formation during postnatal growth and in fracture repair. Mech Dev 71:65–76
6. Bais M et al (2009) Transcriptional analysis of fracture healing and the induction of embryonic stem cell-related genes. PLoS One 4(5):e5393
7. Phillips AM (2005) Overview of the fracture healing cascade. Injury 36S:55–57
8. Buckwalter JA, Einhorn TA, Marsh JL (2001) Bone and joint healing. In: Bucholz RW, Heckman JD (eds) Rockwood and green's fractures in adults. Lippincott Williams and Wilkins pp, Philadelphia, pp 245–271
9. Gerstenfeld LC et al (2003) Impaired fracture healing in the absence of TNF-alpha signaling: the role of TNF-alpha in endochondral cartilage resorption. J Bone Miner Res 18(9): 1584–1592
10. Gardner TN et al (2000) The influence of mechanical stimulus on the pattern of tissue differentiation in a long bone fracture: an FEM study. J Biomech 33:415–425
11. Axelrad TW, Einhorn TA (2011) Use of clinical assessment tools in the evaluation of fracture healing. Injury 42(3):301–305
12. Bhandari M et al (2002) A lack of consensus in the assessment of fracture healing among orthopaedic surgeons. J Orthop Trauma 16(8):562–566
13. Goldhahn J et al (2008) Clinical evaluation of medicinal products for acceleration of fracture healing in patients with osteoporosis. Bone 43:343–347
14. Bouxsein ML et al (2010) Guidelines for assessment of bone microstructure in rodents using micro-computed tomography. J Bone Miner Res 25(7):1468–1486
15. Morgan EF et al (2009) Micro-computed tomography assessment of fracture healing: relationships among callus structure, composition, and mechanical function. Bone 44:335–344
16. Hayward LN et al (2012) MRT letter: Contrast-enhanced computed tomographic imaging of soft callus formation in fracture healing. Microsc Res Tech 75(1):7–14
17. Duvall CL et al (2004) Quantitative microcomputed tomography analysis of collateral vessel development after ischemic injury. Am J Physiol Heart Circ Physiol 287:H302–H310
18. Duvall CL et al (2007) Impaired angiogenesis, early callus formation, and late stage remodeling in fracture healing of osteopontin-deficient mice. J Bone Miner Res 22:286–297
19. Morgan EF et al (2012) Vascular development during distraction osteogenesis proceeds by

sequential intramuscular arteriogenesis followed by intraosteal angiogenesis. Bone 51:535–545

20. Li W et al (2006) High-resolution quantitative computed tomography demonstrating selective enhancement of medium-size collaterals by placental growth factor-1 in the mouse ischemic hindlimb. Circulation 113: 2445–2453
21. Fei J et al (2010) Imaging and quantitative assessment of long bone and vasculature. Microsc Res Tech 293:215–224
22. Schneider PK et al (2009) Simultaneous 3D visualization and quantification of murine bone and bone vasculature using micro-computed tomography and vascular replica. Microsc Res Tech 72:690–701
23. Sider KL, Song J, Davies JE (2010) A new bone vascular perfusion compound for the simultaneous analysis of bone and vasculature. Microsc Res Tech 73:665–672
24. Foux A, Black RC, Uhthoff HK (1990) Quantitative measures for fracture healing: an in-vitro biomechanical study. J Biomech Eng 112:401–406
25. Tsiridis E et al (2007) Effects of OP-1 and PTH in a new experimental model for the study of metaphyseal bone healing. J Orthop Res 25:1193–1203
26. Ulrich-Vinther M, Andreassen TT (2005) Osteoprotegerin treatment impairs remodeling and apparent material properties of callus tissue without influencing structural fracture strength. Calcif Tissue Int 76:280–286
27. Leong PL, Morgan EF (2008) Measurement of fracture callus material properties via nanoindentation. Acta Biomater 4(5):1569–1575
28. Manjubala I (2009) Spatial and temporal variations of mechanical properties and mineral content of the external callus during bone healing. Bone 45:185–192
29. Parfitt AM et al (1987) Bone histomorphometry: standardization of nomenclature, symbols and units. J Bone Miner Res 2:595–610
30. Gerstenfeld LC et al (2005) Perspective: the application of histomorphometric methods to the study of bone repair. J Bone Miner Res 20:1715–1722
31. Gerstenfeld LC et al (2006) Three dimensional reconstruction of fracture callus morphogenesis demonstrates asymmetry in callus development. J Histochem Cytochem 54(11):1215–1228
32. Hacker SA et al (1997) A methodology for the quantitative assessment of articular cartilage histomorphometry. Osteoarthritis Cartilage 5:343–355
33. O'Driscoll SW et al (1999) Method for automated cartilage histomorphometry. Tissue Eng 5:13–23
34. Kon T et al (2001) Expression of osteoprotegerin, receptor activator of NF-kappaB ligand (osteoprotegerin ligand) and related proinflammatory cytokines during fracture healing. J Bone Miner Res 16(6):1004–1014
35. Tiyapatanaputi P et al (2004) A novel murine segmental femoral graft model. J Orthop Res 22:1254–1260
36. Jepsen KJ et al (2008) Genetic variation in the patterns of skeletal progenitor cell differentiation and progression during endochondral bone formation affects the rate of fracture healing. J Bone Miner Res 23(8):1204–1216
37. Kakar S et al (2007) Enhanced chondrogenesis and Wnt-signaling in parathyroid hormone treated fractures. J Bone Miner Res 22(12): 1903–1912
38. Salisbury Palomares KT et al (2010) Transcriptional profiling and biochemical analysis of mechanically induced cartilaginous tissues in a rat model. Arthritis Rheum 62(4):1108–1118
39. Hadjiargyrou M et al (2002) Transcriptional profiling of bone regeneration. Insight into the molecular complexity of wound repair. J Biol Chem 277(33):30177–30182
40. Wang K et al (2006) Analysis of fracture healing by large-scale transcriptional profile identified temporal relationships between metalloproteinase and ADAMTS mRNA expression. Matrix Biol 25(5):271–281
41. Rundle CH (2006) Microarray analysis of gene expression during the inflammation and endochondral bone formation stages of rat femur fracture repair. Bone 38(4):521–529
42. Wise JK et al (2010) Temporal gene expression profiling during rat femoral marrow ablation-induced intramembranous bone regeneration. PLoS One 5(10):e12987
43. Grimes R et al (2011) The transcriptome of fracture healing defines mechanisms of coordination of skeletal and vascular development during endochondral bone formation. J Bone Miner Res 26(11):2597–2609
44. Matsubara H et al (2012) Vascular tissues are a primary source of BMP2 expression during bone formation induced by distraction osteogenesis. Bone 51(1):168–180

http://www.springer.com/978-1-62703-988-8

Skeletal Development and Repair
Methods and Protocols
Hilton, M.J. (Ed.)
2014, X, 328 p. 78 illus., 40 illus. in color., Hardcover
ISBN: 978-1-62703-988-8
A product of Humana Press